Temperature and RyR1 Regulate the Activation Rate of Store-Operated Ca^{2+} Entry Current in Myotubes

Viktor Yarotskyy and Robert T. Dirksen*
Department of Pharmacology and Physiology, University of Rochester Medical Center, Rochester, New York

ABSTRACT Store-operated calcium entry (SOCE) is an important Ca^{2+} entry pathway in skeletal muscle. However, direct electrophysiological recording and full characterization of the underlying SOCE current in skeletal muscle cells (I_{SkCRAC}) has not been reported. Here, we characterized the biophysical properties, pharmacological profile, and molecular identity of I_{SkCRAC} in skeletal myotubes, as well as the regulation of its rate of activation by temperature and the type I ryanodine receptor (RyR1). I_{SkCRAC} exhibited many hallmarks of Ca^{2+} release activated Ca^{2+} currents (I_{CRAC}): store dependence, strong inward rectification, positive reversal potential, limited cesium permeability, and sensitivity to SOCE channel blockers. I_{SkCRAC} was reduced by siRNA knockdown of stromal interaction molecule 1 and expression of dominant negative Orai1. Average I_{SkCRAC} current density at −80mV was 1.00 ± 0.05 pA/pF. In the presence of 20 mM intracellular EGTA, I_{SkCRAC} activation occurred over tens of seconds during repetitive depolarization at 0.5Hz and was inhibited by treatment with 100 μM ryanodine. The rate of SOCE activation was reduced threefold in myotubes from RyR1-null mice and increased 4.6-fold at physiological temperatures (35–37°C). These results show that I_{SkCRAC} exhibits similar biophysical, pharmacological, and molecular properties as I_{CRAC} in nonexcitable cells and its rate of activation during repetitive depolarization is strongly regulated by temperature and RyR1 activity.

INTRODUCTION

Ca^{2+} plays a central role in a multitude of cellular events. Depending on cell type, entry of extracellular Ca^{2+} into the cell can occur through several distinct pathways, including but not limited to, voltage-gated Ca^{2+} channels, receptor-operated Ca^{2+} channels, and store-dependent pathways, including Ca^{2+} release activated Ca^{2+} (CRAC) channels in nonexcitable cells (1) and store-operated calcium entry (SOCE) channels in skeletal (2–5), cardiac (6), and smooth (7) muscle cells.

The molecular structure of CRAC/SOCE channels consists of four pore forming-plasma membrane Orai1 subunits gated by Ca^{2+} store sensor stromal interaction molecule 1 (STIM1) proteins located in the sarco- (SR) or endoplasmic reticulum (1). Although Orai1 and STIM1 proteins are required to form fully functional SOCE channels within the transverse tubule system of skeletal muscle cells (4,8,9), other factors and proteins that influence Ca^{2+} store depletion, STIM1 Ca^{2+} sensitivity, and Orai1 channel activation may regulate SOCE in skeletal muscle. For example, SOCE dysfunction and an increase in muscle fatigability are observed in skeletal muscle cells lacking either mitsugumin29 (MG29) or both the type 1 and type 3 ryanodine receptors (RyR1 and RyR3, respectively) (3).

Prior measurements of SOCE in skeletal muscle cells have primarily been conducted using indirect methods (e.g., rates of Ca^{2+} entry and Mn^{2+} quench using Ca^{2+} sensitive dyes). More direct electrophysiological characterization of SOCE in skeletal muscle remains controversial. Initial attempts to measure single SOCE channel activity in skeletal muscle fibers resulted in a detection of a channel with a conductance of 7–8 pS (10). However, substantial activity of these channels was observed under basal conditions and channel open probability was increased only ~4-fold following SR Ca^{2+} depletion. In addition, these channels were recorded from the pipette-accessible surface membrane (not within the transverse tubule system) and exhibited a weak sensitivity to SOCE/CRAC channels blockers (10). Thus, the actual identity of the 7–8 pS channels remains unclear. A more recent study failed to detect either single channel or whole-cell SOCE currents in adult mouse skeletal muscle fibers, challenging the physiological significance of SOCE in skeletal muscle (11). Thus, direct electrophysiological recording of SOCE channel activity in muscle cells, as well as a rigorous biophysical, pharmacological, and molecular characterization of the underlying current is needed.

In addition to being a Ca^{2+} store sensor, STIM1 was also recently shown to serve as a temperature sensor (12). Specifically, STIM1 multimerization and Orai1 channel coupling is strongly temperature dependent such that a transient increase in temperature promotes STIM1 clustering that can lead to SOCE channel activation upon cooling. Measurement of SOCE channel currents in muscle cells at physiological temperatures has not been reported, which has significantly limited progress in elucidating the physiological role, biophysical properties, and activation rate of SOCE in skeletal muscle. In addition, SOCE dysfunction may contribute to muscle fatigue (3), muscle weakness in aging (13,14), muscular dystrophy (15), and the pathophysiology of malignant hyperthermia (MH) (16,17), a potentially

Submitted November 22, 2011, and accepted for publication June 4, 2012.
*Correspondence: robert_dirksen@urmc.rochester.edu
Editor: David Yue.

0006-3495/12/07/0202/10 $2.00
http://dx.doi.org/10.1016/j.bpj.2012.06.001

deadly pharmacogenic disorder in which volatile anesthetics and depolarizing relaxants trigger uncontrolled muscle contractions in susceptible individuals that occur coincident with a dramatic rise in core body temperature (18). Given this backdrop, direct biophysical and pharmacological characterization of the underlying SOCE current in skeletal muscle cells and assessment of its regulation by physiological factors including repetitive stimulation, temperature, and RyR1 function is of critical importance.

We hypothesized that the rate of SOCE activation depends on SR depletion, which is regulated by temperature and RyR1 Ca^{2+} release during repetitive stimulation. To evaluate the validity of this hypothesis, we used the whole-cell patch clamp technique to directly monitor the biophysical/pharmacological properties and kinetics of activation of the macroscopic Ca^{2+} release-activated Ca^{2+} current in skeletal muscle myotubes derived from normal and RyR1-null mice (referred to here as I_{SkCRAC}). I_{SkCRAC} was activated by promoting store depletion through the use of repetitive voltage clamp depolarization under conditions in which SR Ca^{2+} reuptake was inhibited (e.g., either by extracellular addition of thapsigargin (Tg), a sarco-endoplasmic reticulum Ca^{2+} ATPase (SERCA) pump inhibitor, or inclusion of a high concentration of intracellular EGTA in the patch pipette internal solution). We also compared I_{SkCRAC} properties and kinetics of activation during repetitive depolarization at room and physiological (~37°C) temperatures. Our results show that activation of I_{SkCRAC} in primary skeletal myotubes during repetitive depolarization depends strongly on both temperature and RyR1 Ca^{2+} release channel function.

MATERIALS AND METHODS

Ethical approval

All animals were housed in a pathogen-free area at the University of Rochester and animal protocols carried out in accordance with procedures reviewed and approved by the local University Committee on Animal Resources.

Primary myotube cultures, siRNA transfection, and nuclear injection of Orai1 mutant cDNA

Myotubes derived from normal and RyR1-null (dyspedic) mice were prepared as previously described (19). Electrophysiological experiments were performed on individual myotubes from 8- to 11-day-old cultures. Transfection of murine STIM1 siRNA (Dahrmacon, Chicago, IL) was conducted 2 days after initial plating of myoblasts using Lipofectamine 2000 (Invitrogen, Carlsbad, CA) and did not produce a detectable change in myotube formation or differentiation (4). Transfection of a scrambled siRNA was used as control. Nuclear injection of myotubes with cDNA (0.1 $\mu g\ \mu l^{-1}$) encoding dominant-negative (E106Q) Orai1 (dnOrai1) was performed 5 days after myoblast plating with patch clamp experiments conducted 3 days later (4). Nuclear injections also included a cDNA encoding CD8 (0.05 $\mu g\ \mu l^{-1}$) to allow for subsequent identification of injected myotubes with CD8 antibody-coated beads (4).

Western blot analysis

Cultured myotubes were harvested 5–6 days after transfection of STIM1 small interfering RNAs (siRNAs). STIM1 protein was separated by sodium dodecyl sulfate polyacrylamide gel electrophoresis on a 10% gel. Nonspecific binding was blocked for 1 h with 5% milk in a Tris-buffered saline containing 0.15% Tween 20 (TBST). Membranes were incubated with a rabbit anti-STIM1 (C-terminal) primary antibody (1:1000; Sigma-Aldrich, St. Louis, MO) for 2 h in TBST containing 5% milk. Mouse anti-glyceraldehyde-3-phosphate dehydrogenase (anti-GAPDH) primary antibody (1:50,000; Ambion, Austin, TX) served as a loading control. Membranes were washed three times with TBST and then incubated with a secondary fluorescent conjugated DyLight antirabbit and antimouse antibodies for STIM1 and GAPDH, respectively (1:10,000; Thermo Scientific, Logan, UT) for 1 h in TBST containing 5% milk. Western blot quantification of STIM1 knockdown was determined by densitometry using a LI-COR Odyssey system and ImageJ 1.45s software (Wayne Rasband, National Institute of Mental Health, Bethesda, MD).

Whole-cell patch clamp recording

The whole-cell patch clamp technique was used to directly monitor I_{SkCRAC} in myotubes. Myotubes were voltage clamped at a holding potential of −80 mV. Recordings started 40 s after entering the whole-cell configuration upon membrane rupture. Significant potassium current was not observed even at the start of whole-cell recording (see +40 mV voltage step shown in Fig. S1 *A* in the Supporting Material). I_{SkCRAC} voltage dependence was obtained using a modification of the ramp protocol used widely for measurement of I_{CRAC} in nonexcitable cells (Fig. S1 *A*). Briefly, myotubes were depolarized every 2 s with a voltage stimulus consisting of a 1 s step to 0 mV (to both trigger depolarization-induced SR Ca^{2+} release and to inactivate Na^+ and T-type Ca^{2+} channels) followed by a 30 ms step to +40 mV (to further inactivate sodium channels and monitor outward leak current), followed by a 200 ms voltage ramp from +100 mV to −100 mV (1 mV/ms). I_{SkCRAC} magnitude was quantified from the end of a 65 ms step to −80 mV at the end of each ramp protocol, a voltage in which contamination due to any unblocked voltage-gated ion channels is minimal. Whole-cell currents were recorded with an Axopatch 200A (Molecular Devices, Sunnyvale, CA) amplifier and filtered at 2 kHz by an inline four-pole Bessel filter. Data were digitized at 8.3 kHz using a DigiData 1200 interface (Molecular Devices). Capacitative currents were minimized (>90%) using the capacitative transient cancellation feature of the amplifier. Cell capacitance (C_m) was determined by integration of the capacity transient resulting from a +10-mV pulse applied from the holding potential and was used to normalize I_{SkCRAC} (pA/pF) obtained from different myotubes. Data were collected at both room (21–23°C, RT) and physiological (35–37°C, PT) temperatures.

Recording solutions

Isolation of Ca^{2+} release-activated Ca^{2+} channel current in skeletal myotubes (I_{SkCRAC}) is complicated by the presence of a number of overlapping voltage-gated ion channels. To minimize contribution of voltage-gated channels, myotubes were bathed in an external recording solution containing (in mM): 138 TEA-methanesulfonate, 10 $CaCl_2$, 10 HEPES, 1 $MgCl_2$, 0.1 nifedipine, pH = 7.4 adjusted with tetraethylammonium-hydroxice (TEA-OH). Patch pipettes (0.5–1.2 Mohm resistance) were filled with an internal solution consisting of (in mM): 140 Cs-methanesulfonate, 10 HEPES, 20 Na-EGTA, 4 $MgCl_2$, pH = 7.4 adjusted with CsOH. For some experiments, a low EGTA internal solution was used that contained (in mM): 132 Cs-methanesulfonate, 10 HEPES, 0.1 Na-EGTA, 10 NaCl, 8 $MgCl_2$, pH = 7.4 adjusted with CsOH. L-type Ca^{2+} currents were blocked by 100 μM nifedipine and identical results were also obtained using either 3 μM nifedipine or 50 μM verapamil (Fig. S2), excluding

effects of nifedipine on steady-state I_{SkCRAC}. In some experiments, the effects of 10 μM 2-aminoethoxydiphenyl borate (2-APB) on I_{SkCRAC} current density recorded at −80 mV was determined in the absence of nifedipine.

Offline data analysis

All data analyses were performed using Clampfit10 (Molecular Devices) and Igor Pro 6 (WaveMetrics, Lake Oswego, OR) software suites. I_{SkCRAC} amplitude was determined by averaging the inward current during 20 ms of the final 65 ms voltage step to −80 mV at the end of each I_{SkCRAC} ramp protocol. The time course of I_{SkCRAC} activation was determined by plotting I_{SkCRAC} amplitude at the end of each I_{SkCRAC} ramp protocol delivered every 2 s. A time-dependent increase in inward current at −80 mV, with little or no change in outward current at +40 mV, was used as a measure of activation of inwardly rectifying I_{SkCRAC} (Fig. S1 *A*). Ramp currents obtained before I_{SkCRAC} activation or the first ramp current elicited upon establishing whole-cell mode were used to subtract initial linear currents from sweeps following I_{SkCRAC} activation. I_{SkCRAC} voltage dependence was obtained from individual 200 ms voltage ramp sweeps (1 mV/ms) elicited during each voltage protocol delivered at 0.5 Hz.

The time for 10% (T10%), 50% (T50%), and 90% (T90%) maximal I_{SkCRAC} activation during repetitive depolarization (0.5 Hz) was used as an index for the speed of channel activation. The maximum rate of I_{SkCRAC} activation $(dI_{Norm}/dt)_{Max}$ was determined from the peak of the differential for the time course of normalized I_{SkCRAC} amplitude. All data are presented as mean ± standard error of mean. Statistical significance ($p < 0.05$) was determined using a Student's two-tailed *t*-test. One-way analysis of variance, and Tukey's post hoc test was used to test for differences among three or more independent groups.

Chemicals

N-(4-(3,5-bis(trifluoromethyl)-1H-pyrazol-1-yl)phenyl)-4-methyl-1,2,3-thiadiazole-5-carboxamide (BTP2) was purchased from Fisher Scientific (Pittsburgh, PA). All other chemicals were purchased from Sigma-Aldrich.

RESULTS

Biophysical, pharmacological, and molecular characterization of I_{SkCRAC} in skeletal myotubes

Direct measurement of SOCE current in skeletal myotubes (I_{SkCRAC}) is complicated by several factors, not the least of which is the presence of multiple potential contaminating voltage-dependent sodium, potassium, and calcium channels (8). We used specifically designed recording solutions and voltage protocols (see Materials and Methods for details) to isolate I_{SkCRAC} in whole-cell voltage clamp experiments in primary mouse myotubes (Fig. S1).

I_{SkCRAC} was activated following depletion of SR Ca^{2+}. Two approaches were used to deplete SR Ca^{2+} and activate I_{SkCRAC} (Fig. 1). In the first approach, I_{SkCRAC} was activated by repetitive ramp depolarizations delivered at 0.5 Hz during application of an extracellular recording solution supplemented with 1 μM Tg, a potent and irreversible inhibitor of SERCA pumps, and 30 mM caffeine (Caff), an RyR agonist (Fig. 1, *A* and *B*). In these experiments, a low EGTA-containing (0.1 mM) patch pipette internal solution was used. In the presence of Tg and Caff, Ca^{2+} released during each depolarization is not recycled back into the SR, resulting in progressive SR depletion with each pulse leading to the activation of SOCE. Under these conditions, a relatively slow activation of an inward current recorded at −80 mV was observed that was inhibited by 10 μM BTP2 (Fig. 1 *A*), a pyrazole derivative that inhibits both CRAC channels (20) and TRPC3/5 channels (21). Following activation with Tg and Caff, the voltage dependence of the BTP2-sensitive macroscopic current exhibited strong inward rectification and a very positive reversal potential (Fig. 1 *B*), similar to that observed for I_{CRAC} in T lymphocytes (22,23). This current in skeletal myotubes is referred to as I_{SkCRAC} based on its dependence on store depletion, strong inward rectification, positive reversal potential, and sensitivity to organic and inorganic SOCE channel blockers (see below).

The second approach used to activate I_{SkCRAC} in myotubes involved inhibition of SR Ca^{2+} reuptake during repetitive ramp depolarization (0.5Hz) by inclusion of a high concentration of a strong Ca^{2+} buffer (20 mM EGTA) in the patch pipette internal solution (Fig. 1, *C* and *D*). Under these recording conditions, a similar time-dependent increase in an inwardly rectifying current was observed at −80 mV and was markedly inhibited by both 10 μM BTP2 and 1 μM Gd^{3+} (Fig. 1, *C* and *D*). Subsequent addition of 1 μM Tg and 10 mM Caff failed to further activate an additional inward current component (Fig. S3), indicating that the two approaches for SOCE activation were not additive. For all subsequent experiments, I_{SkCRAC} was activated using the high internal EGTA approach to abrogate global calcium-dependent cytosolic events that could potentially lead to Ca^{2+}-dependent inactivation of SOCE (1).

It is well established that monovalent cations, including Cs^+ ions, readily permeate TRPC and voltage-gated Ca^{2+} channels in the absence of divalent cations (24–26). However, a unique feature of Orai1 channels in nonexcitable cells is that they possess a narrow pore (1) that is poorly permeable to Cs^+ ions in the absence of extracellular divalent cations (27,28). To determine if this unique permeation property is also a feature of SOCE channels in myotubes, we determined the effect of exchanging 155 mM extracellular Cs^+ for 10 mM extracellular Ca^{2+} and 138 mM TEA^+ on I_{SkCRAC} amplitude (Fig. 1, *E* and *F*). Exchange of extracellular Cs^+ for Ca^{2+} and TEA^+ resulted in a rapid, near complete, and fully reversible inhibition of I_{SkCRAC} recorded at −80 mV. The results presented in Fig. 1 indicate that the biophysical properties of I_{SkCRAC} in myotubes are similar to that of I_{CRAC} in T lymphocytes.

The magnitude and pharmacological profile of the time-dependent inward current recorded at −80 mV is summarized in Fig. 2. Specifically, I_{SkCRAC} recorded at −80 mV was significantly inhibited by 5 μM and 10 μM BTP2 (Fig. 2 *A*), 1 μM and 100 μM Gd^{3+} (Fig. 2 *B*), 10 μM

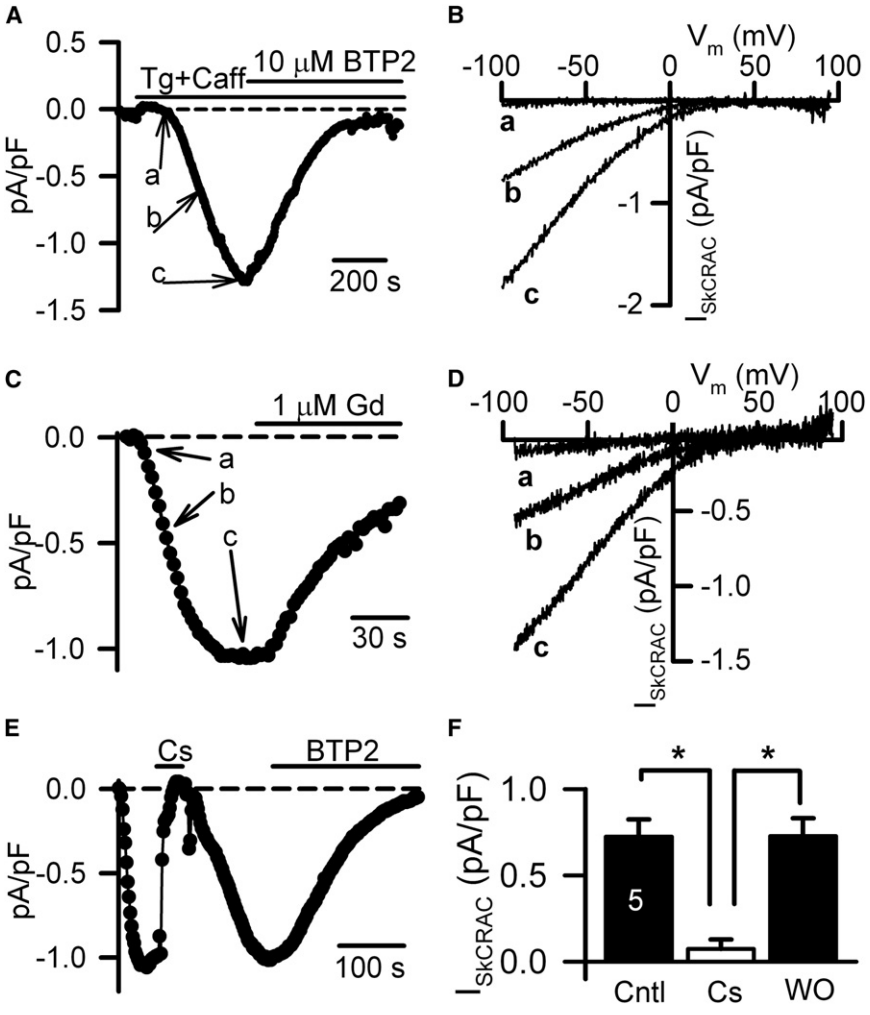

FIGURE 1 Activation time course and biophysical properties of I_{SkCRAC} in normal myotubes. (*A* and *C*) Representative time courses for I_{SkCRAC} activation measured at −80 mV during repetitive ramp depolarization delivered at 0.5 Hz. (*B* and *D*) Representative voltage dependence of I_{SkCRAC} for the times indicated in panels *A* and *C*. (*A*) Time course for I_{SkCRAC} activation during repetitive ramp depolarization during application of 1 μM Tg and 30 mM Caff in the presence of a low EGTA-containing pipette internal solution. Following full activation, I_{SkCRAC} was blocked by addition of 10 μM BTP2. Arrows show time points a, b, and c, used to illustrate I_{SkCRAC} voltage dependence as depicted in panel *B*. The dashed line represents the zero current level and solid lines show the time of drug application. (*B*) Strong inwardly rectifying voltage dependence of I_{SkCRAC} for the time points shown in panel *A*. (*C*) Time course for I_{SkCRAC} activation during repetitive ramp depolarization in the presence of 20 mM EGTA in the patch pipette internal solution. Following full activation, I_{SkCRAC} was blocked by addition of 1 μM Gd^{3+}. Arrows show time points a, b, and c, used to illustrate I_{SkCRAC} voltage dependence as depicted in panel *D*. The dashed line represents the zero current level and solid line shows the time of Gd^{3+} application. (*D*) Strong inwardly rectifying voltage dependence of I_{SkCRAC} for the time points shown in panel *C*. (*E*) Representative time course for I_{SkCRAC} activation recorded at −80 mV under control conditions (10 mM Ca^{2+}), following replacement with 155 mM Cs^{+} (*first solid line*), and following blockade with 10 μM BTP2 (*second solid line*). (*F*) Bar graph depicting average (±SE) I_{SkCRAC} current density recorded at −80 mV in control solution (Cntl, *black bar*), in the presence of 155 mM Cs^{+} external solution, and after washout with control external solution. $^{*}p < 0.05$.

2-APB (Fig. 2 *C*, *left*), and 20 μM SKF 96365 (Fig. 2 *C*, *right*). Interestingly, in contrast to I_{CRAC} in nonexcitable cells, I_{SkCRAC} in myotubes exhibited ~100-fold lower sensitivity to Gd^{3+} block (29,30). Data obtained from all experiments in control myotubes revealed that average I_{SkCRAC} current density recorded at −80 mV was 1.00 ± 0.05 pA/pF ($n = 90$). Histogram analysis of I_{SkCRAC} current density at −80 mV from these experiments exhibited a normal Gaussian distribution with a peak at −0.89 pA/pF and a standard deviation of 0.70 pA/pF (Fig. 2 *D*).

A unique feature of CRAC channels is that low concentrations of 2-APB (e.g., 2–5 μM) increase channel activity, whereas higher concentrations ($\geq$10 μM) produce a transient increase followed by a sustained inhibition (23). Surprisingly, under our standard recording conditions, low concentrations of 2-APB (2 μM and 10 μM) failed to activate I_{SkCRAC} in myotubes (Fig. 2 *C* and Fig. S4, *C–F*). The absence of 2-APB activation under these conditions did not depend on whether I_{SkCRAC} was activated by addition of Tg plus Caff or dialysis of a high concentration of internal EGTA (Fig. S4 *F*). However, we found that 10 μM 2-APB caused a transient facilitation of I_{SkCRAC} current density (recorded at −80 mV) before a subsequent sustained inhibition when the current was measured in the absence of nifedipine (Fig. S4, *A* and *B*). Under these conditions, 10 μM 2-APB produced a similar biphasic modulation of I_{SkCRAC} as that observed for I_{CRAC} in T-lymphocytes channels (23). In contrast, the relatively low sensitivity of I_{SkCRAC} to Gd^{3+} block was not increased in the absence of nifedipine (data not shown).

The low sensitivity to Gd^{3+} block indicates that the molecular determinants of I_{CRAC} and I_{SkCRAC} may be different. However, similar to I_{CRAC} in T lymphocytes, I_{SkCRAC} in myotubes was also inhibited by both siRNA-mediated STIM1 knockdown and the expression of dominant negative E106Q Orai1 (Fig. 3). Specifically, transfection of myotubes with STIM1 siRNAs resulted in a comparable reduction in both STIM1 protein and I_{SkCRAC}

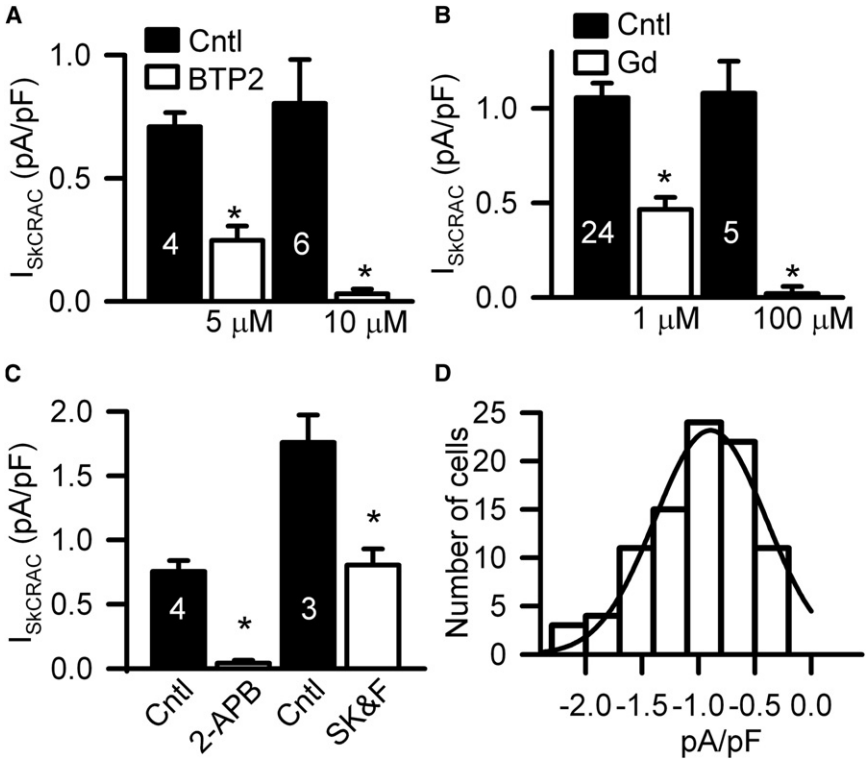

FIGURE 2 I_{SkCRAC} current density and pharmacology. (*A*) Bar graph depicting average (±SE) I_{SkCRAC} current density recorded at −80 mV in control (Cntl, *black bars*) and after addition of either 5 μM or 10 μM BTP2 (BTP2, *open bars*). Numbers of paired experiments are shown in bars. *$p < 0.05$. (*B*) Bar graph depicting average (±SE) I_{SkCRAC} current density recorded at −80 mV in control (Cntl, *black bars*) and after addition of either 1 μM or 100 μM gadolinium (Gd, *open bars*). *$p < 0.05$. (*C*) Bar graph depicting average (±SE) I_{SkCRAC} current density recorded at −80 mV in control (Cntl, *black bars*) and after addition of either 10 μM 2-APB or 20 μM SKF 96365. *$p < 0.05$. (*D*) Histogram distribution of all control peak I_{SkCRAC} current densities measured at −80 mV. The distribution was fitted by a single Gaussian function with a peak value centered at −0.89 pA/pF and a standard deviation of 0.7 pA/pF.

current density measured at −80 mV (Fig. 3, *A* and *B*), whereas I_{SkCRAC} current density was undetectable in E106Q-expressing myotubes (Fig. 3, *C* and *D*). These results show that STIM1-Orai1 coupling underlies I_{SkCRAC} activity in myotubes.

Together, the results presented in Figs. 1–3 indicate that I_{SkCRAC} in primary skeletal myotubes exhibits similar, though not identical, biophysical, pharmacological, and molecular characteristics as those observed for I_{CRAC} in T lymphocytes (22,23).

Rate of I_{SkCRAC} activation is regulated by RyR1 activity

RyR1 plays an essential role in SR Ca^{2+} release during excitation-contraction (EC) coupling (19) and is proposed to

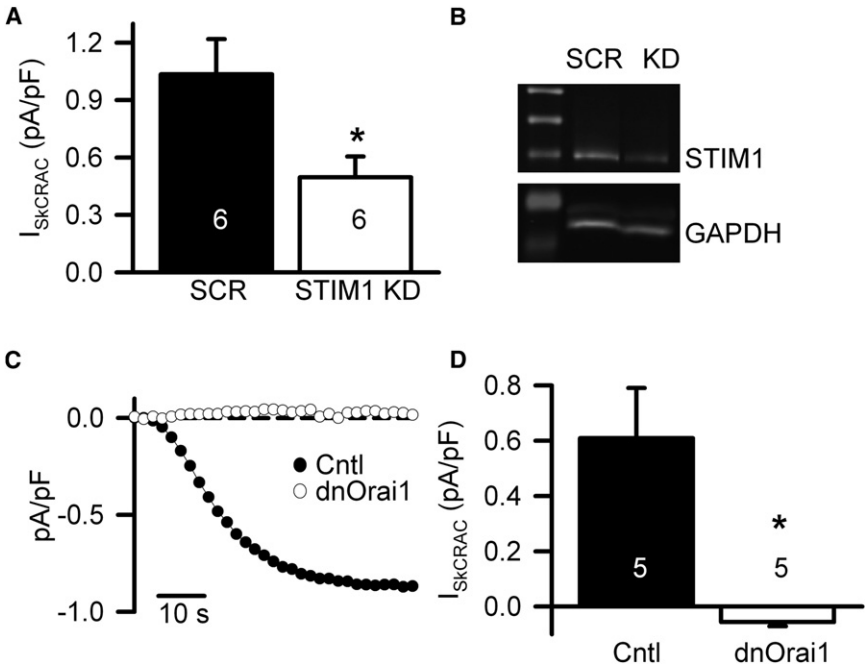

FIGURE 3 STIM1-Orai1 coupling underlies I_{SkCRAC} activity in myotubes. (*A*) Bar graph depicting average (±SE) I_{SkCRAC} current density recorded at −80 mV from myotubes transfected with either scramble (SCR, *black bar*) or STIM1 siRNAs (STIM1 KD, *open bar*). Data were obtained from 5 cells for each group. *$p < 0.05$. (*B*) Western blot analysis for the culture used for the experiments in *A* showing STIM1 expression (*upper*) in myotubes treated with SCR or STIM1 siRNA (KD). GAPDH (*lower*) was used as a loading control. (*C*) Representative time courses for I_{SkCRAC} activation measured at −80 mV during repetitive ramp depolarization (0.5 Hz) obtained from a control (Cntl) myotube and a myotube expressing E106Q dominant negative Orai1 (dnOrai1). (*D*) Bar graph depicting average (± SE) I_{SkCRAC} current density recorded at −80 mV from control myotubes (Cntl, *black bar*) and myotubes expressing dnOrai1 (dnOrai1, *open bar*). Data collected from 5 cells for each group. *$p < 0.05$.

also play an important role in the regulation of SOCE in skeletal myotubes (3,4,31). However, prior studies only indirectly assessed the role of RyRs on SOCE. We found that I_{SkCRAC} was not activated by repetitive 0.5 Hz depolarization in the presence of 0.1 mM EGTA and the absence of SERCA blockade, though subsequent addition of Tg during 0.5 Hz stimulation resulted in the eventual activation of I_{SkCRAC} (Fig. S5). Thus, we compared I_{SkCRAC} magnitude, voltage dependence, and rate of activation under conditions that manipulate RyR functionality and prevent SR Ca^{2+} reuptake (Figs. 4 and 5). First, I_{SkCRAC} activation in the presence of high internal EGTA required repetitive ramp depolarization as no inward current at −80 mV developed over several minutes in the absence of repetitive depolarization (Fig. 4 *A*; $n = 4$), whereas a robust BTP2-sensitive inwardly rectifying current (Fig. 4 *C*; $n = 4$) was readily observed during this time frame in the presence of 0.5 Hz stimulation. Similarly, I_{SkCRAC} activation was not observed during >2 min of repetitive ramp depolarization when RyRs were blocked by pretreating myotubes with 100 μM ryanodine for 1 h (Fig. 4 *B*; $n = 4$). Together, these results indicate that RyR-dependent Ca^{2+} release during repetitive depolarization is required for time-dependent I_{SkCRAC} activation in the presence of high internal EGTA (Fig. 4 *D*).

To more specifically evaluate the role of RyR1 in I_{SkCRAC} activation during repetitive depolarization, we compared the magnitude and rate of I_{SkCRAC} activation in myotubes derived from RyR1-null (dyspedic) and littermate control mice (Fig. 5 *A*). First of all, peak I_{SkCRAC} current density induced by repetitive ramp depolarization in the presence of high EGTA was significantly reduced in RyR1-deficient myotubes (Fig. 5 *B*), consistent with prior reports (3,4). Even more impressively, compared to control myotubes, the rate of I_{SkCRAC} activation during repetitive ramp depolarization was remarkably slowed (~10-fold) in dyspedic myotubes (Fig. 5 *C* and *D*). The dramatic delay in I_{SkCRAC} activation in dyspedic myotubes was assessed from the times for 10% (T10%), 50% (T50%), and 90% (T90%) activation of maximal I_{SkCRAC}. T10%, T50%, and T90% were on average 15-, 8.4-, and 4.5-fold longer, respectively, in dyspedic myotubes (Table S1). The maximum speed of I_{SkCRAC} activation was approximated by taking the peak of the first derivative of the normalized I_{SkCRAC} activation time course (i.e., $(dI_{Norm}/dt)_{Max}$). The maximal speed of I_{SkCRAC} activation was significantly ($p < 0.05$) reduced in dyspedic myotubes (Fig. 5 *D*). Thus, both I_{SkCRAC} magnitude and maximum rate of channel activation during repetitive ramp depolarization were significantly reduced in RyR1-deficient myotubes. Together, the results in Figs. 4 and 5 indicate that RyR1 Ca^{2+} release plays an important role in the magnitude and activation of I_{SkCRAC} during repetitive depolarizations, which is likely to have important physiological implications during prolonged high frequency stimulation of skeletal muscle (see Discussion).

Rate of I_{SkCRAC} activation is increased at physiological temperature

Because STIM1 multimerization is strongly temperature dependent (12) and SOCE dysfunction has been implicated in malignant hyperthermia (16,17), we hypothesized that the rate of I_{SkCRAC} activation during repetitive depolarization is increased at elevated temperatures. To test the validity of this hypothesis, we compared I_{SkCRAC} magnitude, voltage dependence, and rate of activation in myotubes at room (RT = 21–23°C) and physiological (PT = 35–37°C) temperatures (Fig. 6). Myotubes from congenic C57Bl6 mice were used for these experiments. The rate of I_{SkCRAC} activation was significantly accelerated in myotubes maintained at a physiological temperature (Fig. 6 *A*). For the experiment shown in Fig. 6 *A*, I_{SkCRAC} at PT is already nearly maximal at the time in which I_{SkCRAC} only becomes

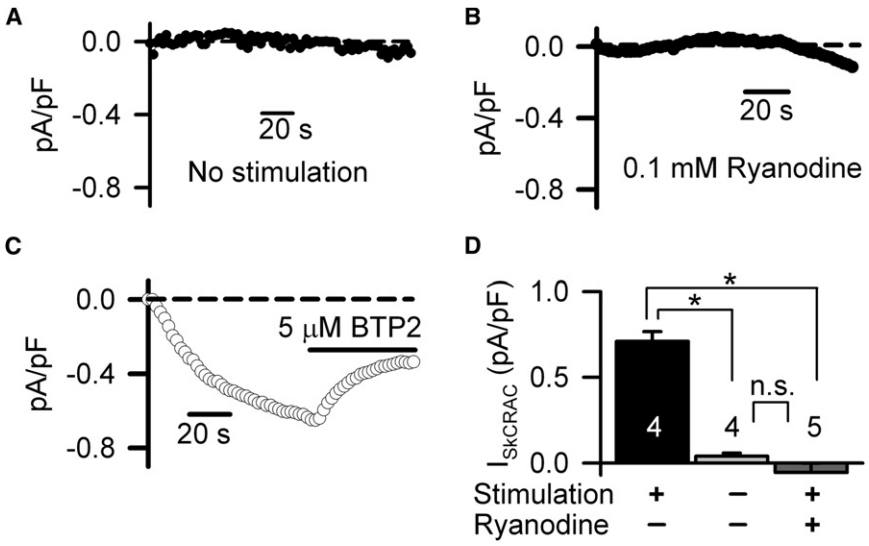

FIGURE 4 RyR1 activity strongly influences I_{SkCRAC} activation during repetitive depolarization. (*A*) Representative time course for I_{SkCRAC} activation at −80 mV in the absence of repetitive (0.5 Hz) ramp depolarization (*no stimulation*). (*B*) Representative time course for I_{SkCRAC} activation at −80 mV observed during repetitive (0.5 Hz) ramp depolarization in the presence of 0.1 mM ryanodine. (*C*) Representative time course for I_{SkCRAC} activation at −80 mV observed during repetitive (0.5 Hz) ramp depolarization in control recording solution and following inhibition with 5 μM BTP2. (*D*) Histogram depicting average (±SE) I_{SkCRAC} current density 60 s after initiation of whole cell recording. Numbers of experiments are shown in bars. Presence of repetitive stimulation and ryanodine are indicated by +.*$p < 0.05$. n.s.; not significantly different.

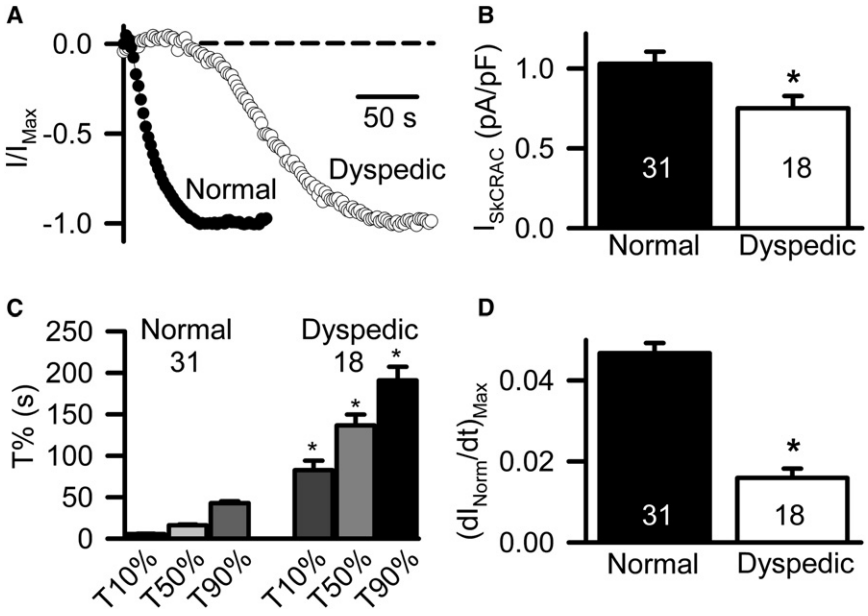

FIGURE 5 I_{SkCRAC} activation during repetitive depolarization is slowed in dyspedic myotubes. (*A*) Representative time courses for activation of normalized I_{SkCRAC} (I/I_{Max}) from normal (*solid circles*) and dyspedic (*open circles*) myotubes. The dashed line represents the zero current level. (*B*) Average (±SE) peak I_{SkCRAC} current density at −80 mV was reduced in dyspedic myotubes. (*C*) The average (±SE) time required for 10% (T10%), 50% (T50%), and 90% (T90%) activation of I_{SkCRAC} was increased for dyspedic myotubes. (*D*) Average (±SE) maximum rate of I_{SkCRAC} activation determined from the peak of the first derivative of the I/I_{Max} time course ($(dI_{Norm}/dt)_{Max}$) was reduced for dyspedic myotubes. *$p < 0.05$.

first detectable at RT (~10 sec). Average values for T10%, T50%, and T90% were all significantly ($p < 0.05$) reduced at PT (Fig. 6 *B* and Table S2), consistent with a strong temperature dependence for I_{SkCRAC} activation. Indeed, the maximal speed of I_{SkCRAC} activation ($[dI_{Norm}/dt]_{Max}$) was >fourfold faster at PT compared to that observed at RT (Fig. 6 *C*). Remarkably, >10% of maximal I_{SkCRAC} was activated by just the second ramp depolarization at PT, resulting in an average T10% slightly <1 s. These results indicate that the formation of functional SOCE channel complexes can be assembled in less than a few hundred milliseconds in myotubes maintained at PT. Maximal I_{SkCRAC} current density was not significantly different between RT and 37°C (0.90 ± 0.11 pA/pF, $n = 7$ and 1.18 ± 0.24 pA/pF, $n = 11$ for RT and PT, respectively), consistent with the total number of activated SOCE channels being similar at these two temperatures. Moreover, the maximum speed of I_{SkCRAC} activation ($(dI_{Norm}/dt)_{Max}$) in dyspedic myotubes was not different at RT and PT, although the time required for 10% (T10%) and 50% (T50%) activation of the current were significantly reduced at PT.

DISCUSSION

Characterization of I_{SkCRAC} in myotubes

The primary objective of this study was to directly measure the SOCE current in myotubes (I_{SkCRAC}) and to characterize

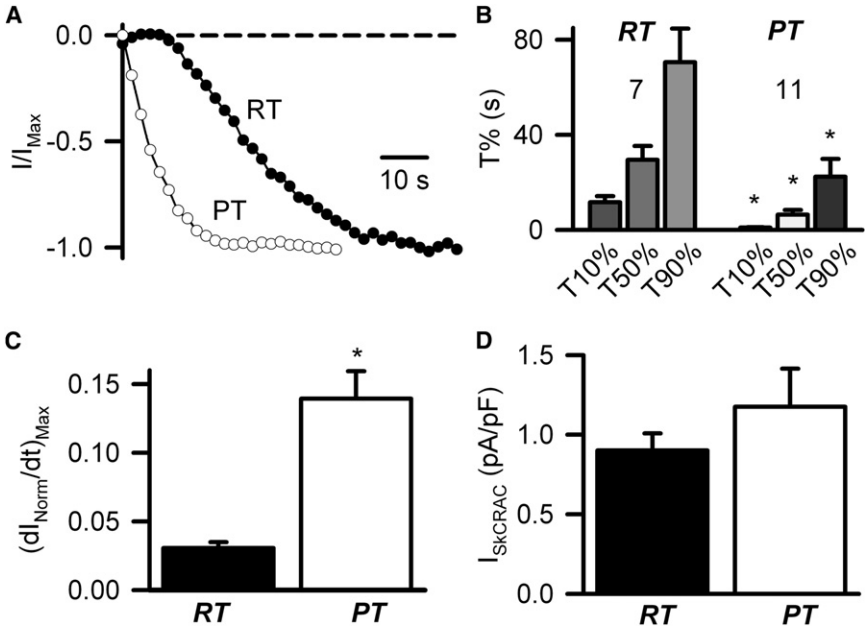

FIGURE 6 Rate of I_{SkCRAC} activation is increased in myotubes at physiological temperature. (*A*) Representative time courses for activation of normalized I_{SkCRAC} (I/I_{Max}) recorded either at room temperature (RT, *solid circles*) or physiological temperature (PT, *open circles*). The dashed line represents the zero current level. (*B*) The average (±SE) time required for 10% (T10%), 50% (T50%), and 90% (T90%) activation of I_{SkCRAC} was reduced at PT. Number of myotubes are indicated in the inset. (*C*) Average (±SE) maximum rate of I_{SkCRAC} activation determined from the peak of the first derivative of the I/I_{Max} time course ($(dI_{Norm}/dt)_{Max}$) was increased at PT. (*D*) Average (±SE) peak I_{SkCRAC} current density recorded at −80 mV was not significantly different between RT and PT. *$p < 0.05$.

the biophysical characteristics, pharmacological profile, and molecular nature of the current. Our measurements of I_{SkCRAC} also enabled us for the first time to characterize the kinetics of SOCE channel activation during repetitive depolarization in muscle cells, as well as its dependence on temperature and RyR activity. Our results show that I_{SkCRAC} activity depends on functional STIM1-Orai1 coupling, and thus the biophysical properties and pharmacological signature of SkCRAC channels in myotubes are similar to that of CRAC channels in T lymphocytes (22,23). Indeed, we show that I_{SkCRAC} in myotubes is activated by store depletion promoted by Ca^{2+} release during repetitive depolarization when SR Ca^{2+} reuptake is inhibited either by prior treatment with Tg or inclusion of a high concentration of EGTA in the patch pipette. Consistent with that observed in T lymphocytes, I_{SkCRAC} current density is relatively small (~1pA/pF at −80 mV), which is ~10–15 times lower than peak L-type Ca^{2+} current density recorded from myotubes under comparable conditions (32). In addition, I_{SkCRAC} recorded in myotubes was significantly reduced by several well-known CRAC channel inhibitors (including BTP2, gadolinium, 2-APB, and SKF96365), exhibited strong inward rectification, a positive reversal potential, low Cs^{+} permeability, and lacked a significant outward current component at strong depolarizations (e.g., +100 mV). The latter result is different than that reported by Stiber et al. (8), the only other study to report electrophysiological measurements of I_{SkCRAC} in myotubes. The reason for this difference is not entirely clear, but may reflect greater leak current during strong depolarization in the prior study.

The bimodal stimulatory and inhibitory effects of 10 μM 2-APB on I_{SkCRAC} in the absence of nifedipine (Fig. S4) is consistent with this current being determined by STIM1-Orai1 coupling. However, an unexpected finding of this study was that transient facilitation of I_{SkCRAC} by 10 μM 2-APB was observed only in the absence of nifedipine. Nifedipine was included in our standard myotube extracellular recoding solution to enable measurement of I_{SkCRAC} voltage dependence in the absence of contaminating L-type Ca^{2+} currents. Nevertheless, time-dependent activation of I_{SkCRAC} during repetitive ramp depolarization in myotubes can be assessed at −80 mV in the absence of nifedipine because L-type Ca^{2+} channels close rapidly (<1 ms) at this potential. To the best of our knowledge, our finding that nifedipine masks 2-APB potentiation of I_{SkCRAC} is the first demonstration of a drug-drug interaction in the pharmacological modulation of STIM1-Orai1 function. Future experiments are needed to determine if nifedipine also masks 2-APB stimulation of CRAC currents in nonmuscle cells and if the effects of nifedipine result from either blocking 2-APB activation or from nifedipine mimicking a sustained 2-APB potentiation of the current.

Despite the similarities between I_{SkCRAC} and I_{CRAC}, one unique SkCRAC channel property was identified in our experiments. I_{SkCRAC} sensitivity to Gd^{3+} block was relatively low, showing only ~50% block at 1 μM and requiring up to 100 μM for complete block. These differences from classic CRAC channel behavior are unexpected given the dependence of I_{SkCRAC} on STIM1-Orai1 coupling. One possible explanation for the unique behavior of I_{SkCRAC} is that Orai1 channels in myotubes are activated in part by coupling to the long splice isoform of STIM1 (STIM1L). Consistent with this idea, McNally et al. (33) recently demonstrated that high Ca^{2+} selectivity and other features of the Orai1 channel pore is conferred by its interaction with STIM1, which could conceivably manifest somewhat differently for STIM1S versus STIM1L.

Our findings here that I_{SkCRAC} depends on store depletion, exhibits strong inward rectification, low Cs^{+} permeability, and is blocked by several known CRAC channel inhibitors validates this current as the direct electrophysiological correlate of SOCE in skeletal myotubes. Previous studies have attempted to record SOCE channel activity in adult skeletal muscle fibers. Ducret et al. (10) used cell-attached patch clamp recordings from the surface membrane of adult flexor digitorum brevis fibers to record single-channel currents that exhibited a linear voltage dependence, a 7–8 picosiemens unitary conductance, and a fourfold increase in open probability following treatment with Tg. However, SOCE channels in adult muscle were subsequently shown to be located deep within the transverse tubule system (34), which is inaccessible to cell-attached patch electrodes. In addition, Orai1 channels exhibit strong inward rectification and a unitary conductance in the femtosiemens range, well below that resolvable by single channel recording. Thus, the single channel currents reported by Ducret et al. were unlikely due to STIM1-Orai1-mediated channel activity in the transverse tubule system. Allard et al. (11) were unable to identify a specific unitary or whole-cell conductance due to store depletion in flexor digitorum brevis fibers isolated from adult mice. Thus, our measurements of I_{SkCRAC} in myotubes provide the first, to our knowledge, complete biophysical, pharmacological, and molecular characterization of SOCE currents in skeletal muscle cells. Although I_{SkCRAC} in myotubes may not directly correlate with the corresponding SOCE channel conductance in adult skeletal muscle fibers, previous measurements of SOCE in adult muscle fibers using indirect imaging approaches have revealed similar molecular and pharmacological properties as those described here. Future work is needed to determine if the electrophysiological approach described here is able to directly measure a similar store-dependent conductance in adult mammalian skeletal muscle fibers.

The type I ryanodine receptor modulates I_{SkCRAC} magnitude and rate of activation

Our results show that RyR1-dependent SR Ca^{2+} depletion triggers activation of SOCE in myotubes because I_{SkCRAC} did not develop in the absence of RyR1 Ca^{2+} release during

EC coupling (i.e., no depolarizations) or when RyR activity was blocked by pretreatment with ryanodine. Our finding that myotube dialysis with a high concentration of EGTA in the absence of stimulation is not sufficient for SOCE activation is in good agreement with the results of Launikonis and Rios (34) who showed that 5 mM BAPTA in zero Ca^{2+} also failed to activate SOCE in fibers in the absence of RyR1 stimulation measured indirectly as Ca^{2+} depletion from sealed t-tubules. In addition, we found that I_{SkCRAC} activation was markedly delayed in dyspedic myotubes, further confirming a role for RyR1 Ca^{2+} release in SOCE activation during repetitive depolarization. The reason for the very slow time-dependent activation of I_{SkCRAC} in EGTA-loaded dyspedic myotubes may reflect an elevated SR Ca^{2+} content in dyspedic myotubes (35), reduced rate of RyR-independent Ca^{2+} leak, or a combination of the two. Alternatively, slow I_{SkCRAC} activation in dyspedic myotubes might result from a low level of SR Ca^{2+} leak through type 3 RyR channels present in myotubes or depolarization-dependent IP_3 production and subsequent IP_3-mediated Ca^{2+} release (36).

Our direct electrophysiological measurements of I_{SkCRAC} confirm a role for RyR1 in depolarization-dependent SOCE channel function in myotubes as reported previously (3). By extension to adult muscle fibers, our results suggest that local store depletion at sites of RyR1 Ca^{2+} release (e.g., SR terminal cisternae) and subsequent activation of SOCE channels in the adjacent t-tubular membrane could occur during prolonged or repetitive high-frequency tetanic stimulation. Moreover, our findings predict that activity-dependent SR Ca^{2+} store depletion, and thus I_{SkCRAC} activation, should be significantly accelerated in muscle cells deficient in calsequestrin1 (see (39)), the major SR Ca^{2+} binding protein in skeletal muscle, or that express MH disease mutations RyR1 that enhance SR Ca^{2+} leak (37,38).

Temperature regulates the rate of I_{SkCRAC} activation

Direct electrophysiological measurements of I_{SkCRAC} in myotubes revealed that SOCE channel activation is a relatively slow process at RT, taking ~1 min for completion during repetitive depolarization at 0.5 Hz (Figs. 5 *C*, 6 *B*, and Tables S1 and S2; see also (8)). However, considerably faster rates of SOCE activation would be expected to occur at higher frequencies of activation (e.g., during 100 Hz tetani) and at more physiological temperatures. Indeed, we found that the maximum rate of I_{SkCRAC} activation observed during 0.5 Hz stimulation was increased >fourfold at physiological temperatures (35–37°C) (Fig. 6 *C* and Table S2). The observed increase in I_{SkCRAC} activation at physiological temperatures could be due to a temperature-dependent increase in either the rate of SR Ca^{2+} depletion, STIM1 multimerization, STIM1/Orai1 coupling, or Ca^{2+} flux through activated Orai1 channels. In this regard, Xaio et al. (12) recently reported that STIM1 multimerization is strongly temperature dependent, which would promote a more rapid assembly of functional STIM1-Orai1 channels and faster I_{SkCRAC} activation. Whatever the underlying mechanism, our demonstration of a strong temperature-dependent increase in the rate of I_{SkCRAC} activation is in good agreement with recent observations that the Ca^{2+} permeability across the surface membrane via SOCE is significantly increased at 39°C in muscle fibers following calsequestrin1 knockdown (39). Thus, future studies are needed to determine the potential role of increased temperature-dependent SOCE activation in the pathophysiology of MH and other heat-related muscle disorders.

CONCLUSION

The presence of SOCE in skeletal muscle is now well established (2–5,8,9,13,14,34,39–42). The potential role of SOCE in regulating the rate of skeletal muscle fatigue (3,8), differentiation (43), its dependence on STIM1 and Orai1 coupling (4,8), regulation by RyRs (3,31), and MG29 (3) have also been reported previously. However, conclusions from all of these studies have hinged almost entirely on indirect measures of SOCE activity (e.g., Ca^{2+} influx, Mn^{2+} quench, change in Ca^{2+} dye fluorescence trapped in t-tubules of mechanically skinned fibers). In this study, we developed a standardized electrophysiological approach to quantify the SOCE current (I_{SkCRAC}) in myotubes, validated the measure according to multiple known biophysical, pharmacological, and molecular SOCE channel properties, and used this direct measure of SOCE channel function to determine the role of temperature and ryanodine receptor functionality on the rate of SOCE channel activation during repetitive activation. The results show that increases in ambient temperature and RyR1 Ca^{2+} release promote I_{SkCRAC} magnitude (RyR1) and rate of activation (RyR1 and temperature) during repetitive stimulation.

SUPPORTING MATERIAL

Two tables and five figures are available at http://www.biophysj.org/biophysj/supplemental/S0006-3495(12)00629-7.

We thank Dr. Keith S Elmslie (Kirksville College of Osteopathic Medicine, A. T. Still University of Health Sciences) for critical review of an early version of this manuscript. We also thank Dr. P. D. Allen for providing access to the dyspedic mice used in this study and to Sara Geitner for superb technical assistance in myotube preparation. We thank Ellie Carrell for help with the Western blot analyses. The authors declare no conflict of interest.

This work was supported by a research grant from the National Institutes of Health (AR059646 to RTD).

REFERENCES

1. Prakriya, M. 2009. The molecular physiology of CRAC channels. *Immunol. Rev.* 231:88–98.
2. Kurebayashi, N., and Y. Ogawa. 2001. Depletion of Ca^{2+} in the sarcoplasmic reticulum stimulates Ca^{2+} entry into mouse skeletal muscle fibres. *J. Physiol.* 533:185–199.

3. Pan, Z., D. Yang, …, J. Ma. 2002. Dysfunction of store-operated calcium channel in muscle cells lacking mg29. *Nat. Cell Biol.* 4:379–383.
4. Lyfenko, A. D., and R. T. Dirksen. 2008. Differential dependence of store-operated and excitation-coupled Ca^{2+} entry in skeletal muscle on STIM1 and Orai1. *J. Physiol.* 586:4815–4824.
5. Launikonis, B. S., M. Barnes, and D. G. Stephenson. 2003. Identification of the coupling between skeletal muscle store-operated Ca^{2+} entry and the inositol trisphosphate receptor. *Proc. Natl. Acad. Sci. USA.* 100:2941–2944.
6. Uehara, A., M. Yasukochi, …, H. Takeshima. 2002. Store-operated Ca^{2+} entry uncoupled with ryanodine receptor and junctional membrane complex in heart muscle cells. *Cell Calcium.* 31:89–96.
7. Albert, A. P., S. N. Saleh, …, W. A. Large. 2007. Multiple activation mechanisms of store-operated TRPC channels in smooth muscle cells. *J. Physiol.* 583:25–36.
8. Stiber, J., A. Hawkins, …, P. Rosenberg. 2008. STIM1 signalling controls store-operated calcium entry required for development and contractile function in skeletal muscle. *Nat. Cell Biol.* 10:688–697.
9. Dirksen, R. T. 2009. Checking your SOCCs and feet: the molecular mechanisms of Ca^{2+} entry in skeletal muscle. *J. Physiol.* 587:3139–3147.
10. Ducret, T., C. Vandebrouck, …, P. Gailly. 2006. Functional role of store-operated and stretch-activated channels in murine adult skeletal muscle fibres. *J. Physiol.* 575:913–924.
11. Allard, B., H. Couchoux, …, V. Jacquemond. 2006. Sarcoplasmic reticulum Ca^{2+} release and depletion fail to affect sarcolemmal ion channel activity in mouse skeletal muscle. *J. Physiol.* 575:69–81.
12. Xiao, B., B. Coste, …, A. Patapoutian. 2011. Temperature-dependent STIM1 activation induces $Ca^{2}+$ influx and modulates gene expression. *Nat. Chem. Biol.* 7:351–358.
13. Thornton, A. M., X. Zhao, …, M. Brotto. 2011. Store-operated $Ca(^{2+})$ entry (SOCE) contributes to normal skeletal muscle contractility in young but not in aged skeletal muscle. *Aging (Albany NY).* 3:621–634.
14. Zhao, X., N. Weisleder, …, M. Brotto. 2008. Compromised store-operated Ca^{2+} entry in aged skeletal muscle. *Aging Cell.* 7:561–568.
15. Millay, D. P., S. A. Goonasekera, …, J. D. Molkentin. 2009. Calcium influx is sufficient to induce muscular dystrophy through a TRPC-dependent mechanism. *Proc. Natl. Acad. Sci. USA.* 106:19023–19028.
16. Duke, A. M., P. M. Hopkins, …, D. S. Steele. 2010. Store-operated Ca^{2+} entry in malignant hyperthermia-susceptible human skeletal muscle. *J. Biol. Chem.* 285:25645–25653.
17. Zhao, X., N. Weisleder, …, J. Ma. 2006. Azumolene inhibits a component of store-operated calcium entry coupled to the skeletal muscle ryanodine receptor. *J. Biol. Chem.* 281:33477–33486.
18. Rosenberg, H., N. Sambuughin, and R. Dirksen. 2010. Malignant hyperthermia susceptibility. *In* GeneReviews at GeneTests: Medical Genetics Information Resource (database online). Copyright, University of Washington, Seattle. 1997–2010.
19. Nakai, J., R. T. Dirksen, …, P. D. Allen. 1996. Enhanced dihydropyridine receptor channel activity in the presence of ryanodine receptor. *Nature.* 380:72–75.
20. Zitt, C., B. Strauss, …, M. Hoth. 2004. Potent inhibition of Ca^{2+} release-activated Ca^{2+} channels and T-lymphocyte activation by the pyrazole derivative BTP2. *J. Biol. Chem.* 279:12427–12437.
21. He, L. P., T. Hewavitharana, …, D. L. Gill. 2005. A functional link between store-operated and TRPC channels revealed by the 3,5-bis(trifluoromethyl)pyrazole derivative, BTP2. *J. Biol. Chem.* 280:10997–11006.
22. Prakriya, M., and R. S. Lewis. 2002. Separation and characterization of currents through store-operated CRAC channels and Mg^{2+}-inhibited cation (MIC) channels. *J. Gen. Physiol.* 119:487–507.
23. Prakriya, M., and R. S. Lewis. 2001. Potentiation and inhibition of $Ca(^{2+})$ release-activated $Ca(^{2+})$ channels by 2-aminoethyldiphenyl borate (2-APB) occurs independently of $IP(_3)$ receptors. *J. Physiol.* 536:3–19.
24. Coronado, R., and J. S. Smith. 1987. Monovalent ion current through single calcium channels of skeletal muscle transverse tubules. *Biophys. J.* 51:497–502.
25. Hess, P., J. B. Lansman, and R. W. Tsien. 1986. Calcium channel selectivity for divalent and monovalent cations. Voltage and concentration dependence of single channel current in ventricular heart cells. *J. Gen. Physiol.* 88:293–319.
26. Salido, G. M., I. Jardín, and J. A. Rosado. 2011. The TRPC ion channels: association with Orai1 and STIM1 proteins and participation in capacitative and non-capacitative calcium entry. *Adv. Exp. Med. Biol.* 704:413–433.
27. McNally, B. A., M. Yamashita, …, M. Prakriya. 2009. Structural determinants of ion permeation in CRAC channels. *Proc. Natl. Acad. Sci. USA.* 106:22516–22521.
28. Bakowski, D., and A. B. Parekh. 2002. Monovalent cation permeability and $Ca(^{2+})$ block of the store-operated $Ca(^{2+})$ current $I(_{CRAC})$in rat basophilic leukemia cells. *Pflugers Arch.* 443:892–902.
29. Yeromin, A. V., S. L. Zhang, …, M. D. Cahalan. 2006. Molecular identification of the CRAC channel by altered ion selectivity in a mutant of Orai. *Nature.* 443:226–229.
30. Ross, P. E., and M. D. Cahalan. 1995. Ca^{2+} influx pathways mediated by swelling or stores depletion in mouse thymocytes. *J. Gen. Physiol.* 106:415–444.
31. Kiselyov, K. I., D. M. Shin, …, S. Muallem. 2000. Gating of store-operated channels by conformational coupling to ryanodine receptors. *Mol. Cell.* 6:421–431.
32. Avila, G., and R. T. Dirksen. 2000. Functional impact of the ryanodine receptor on the skeletal muscle L-type $Ca(^{2+})$ channel. *J. Gen. Physiol.* 115:467–480.
33. McNally, B. A., A. Somasundaram, …, M. Prakriya. 2012. Gated regulation of CRAC channel ion selectivity by STIM1. *Nature.* 482:241–245.
34. Launikonis, B. S., and E. Ríos. 2007. Store-operated Ca^{2+} entry during intracellular Ca^{2+} release in mammalian skeletal muscle. *J. Physiol.* 583:81–97.
35. Kimura, T., J. D. Lueck, …, A. F. Dulhunty. 2009. Alternative splicing of RyR1 alters the efficacy of skeletal EC coupling. *Cell Calcium.* 45:264–274.
36. Estrada, M., C. Cárdenas, …, E. Jaimovich. 2001. Calcium transients in 1B5 myotubes lacking ryanodine receptors are related to inositol trisphosphate receptors. *J. Biol. Chem.* 276:22868–22874.
37. Chelu, M. G., S. A. Goonasekera, …, S. L. Hamilton. 2006. Heat- and anesthesia-induced malignant hyperthermia in an RyR1 knock-in mouse. *FASEB J.* 20:329–330.
38. Durham, W. J., P. Aracena-Parks, …, S. L. Hamilton. 2008. RyR1 S-nitrosylation underlies environmental heat stroke and sudden death in Y522S RyR1 knockin mice. *Cell.* 133:53–65.
39. Zhao, X., C. K. Min, …, J. Ma. 2010. Increased store-operated Ca^{2+} entry in skeletal muscle with reduced calsequestrin-1 expression. *Biophys. J.* 99:1556–1564.
40. Takekura, H., M. Nishi, …, C. Franzini-Armstrong. 1995. Abnormal junctions between surface membrane and sarcoplasmic reticulum in skeletal muscle with a mutation targeted to the ryanodine receptor. *Proc. Natl. Acad. Sci. USA.* 92:3381–3385.
41. Yang, T., P. D. Allen, …, J. R. Lopez. 2007. Enhanced excitation-coupled calcium entry in myotubes is associated with expression of RyR1 malignant hyperthermia mutations. *J. Biol. Chem.* 282:37471–37478.
42. Shin, D. W., Z. Pan, …, J. Ma. 2003. A retrograde signal from calsequestrin for the regulation of store-operated Ca^{2+} entry in skeletal muscle. *J. Biol. Chem.* 278:3286–3292.
43. Darbellay, B., S. Arnaudeau, …, L. Bernheim. 2009. STIM1- and Orai1-dependent store-operated calcium entry regulates human myoblast differentiation. *J. Biol. Chem.* 284:5370–5380.